A DIRECT METHOD FOR SOLVING CRACK GROWTH PROBLEMS—I

X. Li and L. M. Keer

Department of Civil Engineering, Northwestern University, Evanston, IL 60208, U.S.A.

Abstract—Based on the boundary element equation approach for crack opening displacements, an equation of the perturbation type is derived giving an explicit relation between the crack front variation and the resulting variation in the stress intensity factor. By using this equation, the crack front advance can be predicted at each step of crack growth while ensuring that the fracture criterion is satisfied for the new crack geometry. As an example, the problem of the growth under a Dugdale-type model for cracks of elliptical and circular shapes with uniform and linear variation of tensile loads is solved and the numerical results are discussed.

INTRODUCTION

For three-dimensional crack problems, most analytical efforts have been concerned with stationary cracks, where the geometry of the crack and the loading conditions are given. Various analytical and numerical methods have been developed to solve such stationary crack problems to determine the crack opening displacement and the stress intensity factor along the crack front.

However, another class of problems, crack growth, although of practical interest in many fields, has not been addressed in a systematic way. The stationary crack problems belong to the traditional direct problems of mechanics in which the geometry is known *a priori*. Crack growth problems on the other hand have the feature that the geometry of the crack is not given and must be determined through the solution procedure. The only requirement for the determination of the new crack front after growth is that the fracture criterion, which is directly related to the stress intensity factor, be satisfied.

This class of problems was addressed previously by using an iteration approach (Mastrojannis *et al.*, 1980; Lee and Keer, 1986, and others). At each step the crack advance was determined by adopting an *ad hoc* fatigue crack growth law analogous to the Paris law. The iteration continued until an equilibrium crack front was found. This method, although pragmatic, is not satisfactory for the following reason: although the fracture criterion is satisfied for the final geometry of the crack, it may be violated during the iteration procedure and hence the searching process may contain error and not represent the actual growth process of the crack and the convergence in general is not guaranteed. Recent examples of applications of this approach appear in the work of Gao and Rice (1989) and Fares (1989).

In recent years Rice (1985, 1987) and Gao and Rice (1986, 1987) have developed a theory for calculating directly the first order variation in crack opening displacement and stress intensity factor due to small changes in crack geometry. Bower and Ortiz (1990) extended this first order perturbation scheme to arbitrarily large variations of crack geometries. By repeated small perturbations applied to some initial geometry, results for cracks of arbitrary shapes were derived. A number of crack growth problems of interest have been solved by this method (Bower and Ortiz, 1990; Li and Keer, 1992). However, there are severe restrictions to the application of this approach to general crack growth problems. Due to the strong singularity contained in the integral in the basic equations, the method can only be applied to cracks in a homogeneous medium with uniform loading conditions.

For solving general crack growth problems, it is necessary to develop equations to which a perturbation approach can give an explicit relation between the crack front variation and the resulting changes in the stress intensity factor. Then, it becomes possible to

determine the crack front advance which will result in a given variation of stress intensity factor such that the fracture criterion is satisfied at each new crack front.

In this paper it is shown how to derive such equations from the boundary integral equation, which is originally developed to solve for the crack opening displacement and the stress intensity factor and in the present analysis is used to solve crack growth problems. It is interesting to note that the concept of deriving the relation between the crack growth and the resulting changes in the stress intensity factor from the corresponding integral equation first appeared in the papers of Nemat-Nasser *et al.* (1978) and Keer *et al.* (1978) for two-dimensional crack growth problems related to the stability of interacting cracks. The quantities in the integral equations are viewed as the functions of the crack lengths. By differentiation, the equation for the derivatives of the stress intensity factor with respect to the crack lengths are obtained and the problem of the stability of the crack growth is addressed. For the three-dimensional problems considered in this paper, the coefficients, as well as the solution of the boundary integral equation, depend upon the shape of the crack. By differentiation with respect to the positions of the nodal points on the crack front, a perturbation type relation can be derived between the nodal point displacement and the variation of the stress intensity factor.

As an application of this method, the growth of the yield zone of a Dugdale-type crack of circular shape under linear variation of load as well as of elliptical shapes under uniform load are solved.

Formulation

Consider planar cracks subjected to tensile forces which induce a mode I stress intensity factor around the crack front. For stationary crack problems with the crack opening displacement Δu as the unknown function, a suitable boundary integral equation, defined on the crack faces, can be established in the form

$$\int K(x, x_0)\Delta u(x)\, dA(x) = -p(x_0),\tag{1}$$

where $K(x, x_0)$ is the kernel function and p is the normal pressure on the crack faces. After putting eqn (1) into a discrete form by a proper numerical scheme, it is reduced to the following set of algebraic equations:

$$H_{ij}\Delta\bar{u}_j = -p_i,\quad i = 1, 2, \ldots, N,\tag{2}$$

where p_i is the pressure at the collocation point x_i; $H_{ij} = \int_{A_j} K(x, x_i)w(x)\, dA$. Here, A_j is the jth subdomain (element) of the crack faces and $w(x)$ is the weight function which describes the variation of Δu within each element:

$$\Delta u(x) = \Delta\bar{u}w(x).\tag{3}$$

Two types of elements are distinguished as follows: the inside element and the crack front element; the latter has an edge or vertex that lies on the crack front. After solving $\Delta\bar{u}$ from eqn (2) the stress intensity factor K is calculated from the crack opening displacement of the crack front elements by the known relation:

$$\Delta u(x_0) = \Delta\bar{u}w(x_0) = \frac{4(1-v)}{\sqrt{2\pi\mu}} K\sqrt{\varepsilon_0},\tag{4}$$

where ε_0 is the distance of point x_0 from the crack front. To obtain an accurate result of the stress intensity factor the asymptotic behavior of Δu near the crack front as shown by the right side of eqn (4) should be incorporated into the expression for the weight function.

With a continuous increase in the applied load, the stress intensity factor at some points along the crack front will eventually reach a critical value, the fracture toughness of

the material, such that any further increment in the load will force the crack to grow. The change of the crack geometry after growth is specified by the crack front displacement, which will cause a perturbation to eqn (1) with the form:

$$\delta \int K(x, x_0) \Delta u(x)\, dA(x) = -\delta p(x_0).$$ (5)

Now the same discretization scheme which is applied to eqn (1) to obtain eqn (2) is used. The crack face is divided into N elements and the function of the crack face opening displacement is approximated by the piecewise function $\Delta \bar{u}_j w(x)$, $j = 1, 2, \ldots, N$. Equation (5) is then reduced to the following discrete form:

$$\sum_{j=1}^{N} \delta \left[\Delta \bar{u}_j \int_{\Delta_j} K(x, x_i) w(x)\, dA \right] = -\delta p(x_i), \quad i = 1, 2, \ldots, N$$ (6)

or

$$H_{ij}\delta(\Delta \bar{u}_j) + \delta H_{ij}\Delta \bar{u}_j = -\delta p_i, \quad i = 1, 2, \ldots, N,$$ (7)

where higher order terms such as $\delta H_{ij}\delta \Delta \bar{u}_j$ are neglected.

For a given approximation scheme the crack front is totally determined by the position of nodal points along the crack front. Consequently for crack growth problems, the variation of the crack geometry during crack growth is specified by the displacements of the nodes on the crack front. In the sequel δa_j will be used to denote the displacement of the jth front node along the direction normal to the crack front. Equation (7) can then be written as

$$H_{ij}\delta(\Delta \bar{u}_j) + \frac{\partial H_{ij}}{\partial \delta a_m} \Delta \bar{u}_j \delta a_m = -\delta p_i, \quad i = 1, 2, \ldots, N.$$ (8)

In the above equation the summation over j is from 1 to N and the summation over m is from 1 to M, where M is the total number of frontal nodes. The term $(\partial H_{ij}/\partial \delta a_m)\delta a_m$ is calculated as

$$\frac{\partial H_{ij}}{\partial \delta a_m}\delta a_m = \frac{\partial H_{ij}}{\partial x_m}\delta x_m + \frac{\partial H_{ij}}{\partial y_m}\delta y_m = \left(\frac{\partial H_{ij}}{\partial x_m} n_{xm} + \frac{\partial H_{ij}}{\partial y_m} n_{ym} \right)\delta a_m,$$ (9)

where $x_m = (x_m, y_m)$ is the position vector of the mth crack front node and $n_m = (n_{xm}, n_{ym})$ is the normal to the crack front at that point. When the crack front is approximated by a polygon, the normal to the crack front at the mth node is taken as the normal to a parabola fitting through the mth node and the two adjacent nodes. From eqn (9) the operator $\partial/\partial \delta a_m$ will be understood in the sequel as

$$\frac{\partial}{\partial \delta a_m} = n_{xm}\frac{\partial}{\partial x_m} + n_{ym}\frac{\partial}{\partial y_m}.$$ (10)

It should be pointed out that for crack front element the variation of Δ_j, the area of the element has to be taken into account when calculating $\partial H_{ij}/\partial \delta a_m$. The calculation of H_{ij} usually involves the evaluation of three different integrals over the jth element whose nodes will be denoted by x_o, x_p and x_q. The calculation of $\partial H_{ij}/\partial \delta a_m$ for these integrals is discussed next.

When $i \neq j$, i.e. when the collocation point x_i is not in the jth element, H_{ij} is usually calculated by a two-dimensional numerical integration scheme, which has the general form:

X. Li and L. M. Keer

$$H_{ij} = \int_{\Delta} K(x, x_i) w(x) \, dA = A(x_i, x_p, x_q) \sum_{k=1}^{N} B_k K(x_k, x_i) w(x_k). \qquad (11)$$

where A is the area of the element and B_k are the integration weights. The integration points are determined from the nodal points x_i, x_p and x_q of the element through a linear relation, $x_k = L_k(x_i, x_p, x_q)$. The collocation points are similarly related to the nodes of the ith element through $x_i = C_i(x_a, x_p, x_q)$.

The derivative of H_{ij} with respect to δa_m has the form

$$\frac{\partial H_{ij}}{\partial \delta a_m} = A(x_i, x_p, x_q) \sum_{k=1}^{N} B_k \left\{ K(x_k, x_i) \left[\frac{\partial w(x_k)}{\partial \delta a_m} + \frac{\partial w(x_k)}{\partial x_k} \frac{\partial L_k}{\partial \delta a_m} \right] + w(x_k) \right.$$

$$\left. \times \left[\frac{\partial K(x_k, x_i)}{\partial x_k} \frac{\partial L_k}{\partial \delta a_m} + \frac{\partial K(x_k, x_i)}{\partial x_i} \frac{\partial C_i}{\partial \delta a_m} \right] \right\} + \frac{\partial A(x_i, x_p, x_q)}{\partial \delta a_m} \sum_{k=1}^{N} B_k K(x_k, x_i) w(x_k). \quad (12)$$

where the term $\partial w(x_k)/\partial \delta a_m$ is produced by the change of distance between the integration point x_k and the crack front, while x_k remains unchanged. It appears that only when the crack front node x_m coincides with one of the three nodes x_a, x_p, x_q that the terms associated with $\partial L_k/\partial \delta a_m$ and $\partial A(x_a, x_p, x_q)/\partial \delta a_m$ exist. The same argument applies to $\partial C_i/\partial \delta a_m$.

When $i = j$, i.e. when the collocation point x_i lies within the jth element, where the integration is to be carried out, then the integral is singular and is calculated by the sum of the following three integrals:

$$H_{ij} = \int_{\Delta_j} K(x, x_i) w(x) \, dA = \int_{\Delta_j} \left[K(x, x_i) - K^*(x, x_i) \right] w(x) \, dA$$

$$+ \text{P.V.} \int_{\Delta_j} K^*(x, x_i) [w(x) - w(x_i)] \, dA + \text{F.P.} w(x_i) \int_{\Delta_j} K^*(x, x_i) \, dA, \quad (13)$$

where K^* is the singular part of the kernel function; P.V. and F.P. indicate Cauchy principal value integral and finite part integral, respectively. The two-dimensional principal value integral is evaluated by a numerical formula, such as the one given by Theocaris *et al.* (1980):

$$\text{P.V.} \int_{\Delta_j} \frac{u(x, x_i)}{r^2} \, dA = \text{P.V.} \int_{\Delta} \frac{u(r, \theta)}{r^2} \, dA$$

$$= \sum_{i=0}^{M-1} \Delta \theta_i B_i \left\{ \left[\sum_{k=1}^{N} A_k u(R(\theta_i) \rho_k, \theta_i) \right] + u(0, \theta_i) \ln R(\theta_i) \right\}. \quad (14)$$

where $u(x, x_i) = r^2 K^*(x, x_i)[w(x) - w(x_i)]$; A_k and B_i are the weights and ρ_k the abscissae; r is the distance between the integration points and the collocation point, and R is the distance of x_i from the boundary of the element. The quantity θ_i is usually related to the positions of the nodes of the element. For inside elements, the crack front advance will affect the variation of the above Cauchy principal value integral only through the variation of $w(x)$ and $w(x_i)$, and the calculation of the derivatives of the integral with respect to δa is straightforward. However, crack front elements which have one or two nodes on the crack front must be treated with care. When differentiating the above equation with respect to δa_m, all the effects of the displacement of the nodal points on the position of x_i and on R and θ_i, directly as well as through the variation of x_i, in addition to the variation of $w(x)$, should be taken into account, which makes the resulting formulae complicated. Due to their length and complexity they are not included in this paper.

The finite part integral generally has a closed form (Lin and Keer, 1987), which depends

on the position of the nodes of the element as well as that of the collocation point:

$$\text{F.P.}w(x_i) \int_{\Delta_i} K^s(x, x_i)\, d\mathcal{A} = w(x_i)F(x_o, x_p, x_q, x_i).$$ (15)

The differentiation of the finite part integral with respect to positions of the collocation points as well as the nodal points is performed by differentiating the right-hand side of the equation. The resulting formulae are given in the Appendix.

For the application to crack growth problems. it is desired to obtain an equation which gives a relation between the crack front advance and the resulting changes in the stress intensity factor. By performing matrix manipulation and incorporating eqn (4) this equation is readily derived from eqn (8) as:

$$A_{ij}\delta a_j = \delta K_i, \quad i = 1, 2, \ldots, M.$$ (16)

where M is the total number of the crack front elements. In deriving eqn (16). δp is taken to be zero in eqn (8). Hence δK in the above equation is solely produced by the crack advance. The variation of stress intensity factor caused by the variation of the load is solved from eqn (8) by letting $\delta a = 0$.

Equation (16) can be used in a variety of ways. The resulting changes in stress intensity factor due to a given crack front advance δa can be calculated. or conversely, the unknown δa which results in a required variation in stress intensity factor. δK. can be determined. Equation (16) can also be employed to solve problems having mixed unknowns. i.e. at some points on the crack front δK is prescribed and at the remaining points δa is specified, such as are encountered in the problem of crack growth between barriers or obstacles.

Equation (16) is solved by incorporating the fracture criterion $K \leqslant K_c$ as an inequality boundary condition on the unknowns.

For crack front elements:

$$\delta K = 0, \quad \delta a \neq 0 \quad \text{if } K = K_c;$$
$$\delta K \neq 0, \quad \delta a = 0 \quad \text{if } K < K_c,$$ (17)

where K_c is the local fracture toughness of the material.

For a general triangulation mesh scheme, the total number of crack front elements exceeds the number of crack front nodes. In such cases, eqn (16) is an overdetermined system of algebraic equations, which is solved as a standard least squares problem as follows: find the solution δa which minimizes the normal of the residual: $\| A\delta a - \delta K \|$ (Bertero et al., 1985).

It is possible to prescribe only δK for those crack front elements which have an edge on the crack front. in order to keep the number of equations equal to the number of the unknown crack front node displacements. However, it is observed in such cases that a small difference in the prescribed δK may result in a large fluctuation in the solution δa, which reflects the unstable character generally associated with the solution of inverse problems. in which the geometry of a problem is to be determined from known information on the stress field. By prescribing δK for all crack front elements, more restrictions are imposed on the unknown crack front node advance, which makes the resulting solution stable.

With the solved unknowns δa. $\delta(\Delta\bar{u})$ and δK from eqns (8) and (16) the new crack front is determined and the crack opening displacement Δu and the stress intensity factor K are updated for the new crack configuration to which the above analysis can then be repeated. Since only first order perturbation is considered in eqn (8). each step of the crack advance has to be kept sufficiently small to ensure the accuracy of the result. However, as the perturbation can be repeated indefinitely by successively updating the crack geometry and the corresponding crack opening displacement and the stress intensity factor, this

method can be used to analyse arbitrarily large deformations of the crack geometry, which simulates the crack growth process.

In the analysis eqn (2) is used to calculate the crack opening displacement $\Delta \bar{u}$ and the stress intensity factor K for the initial crack geometry. After a number of perturbation steps eqn (2) may be used again to calculate $\Delta \bar{u}$ and K of the perturbed crack in order to prevent the possible accumulation of errors in the perturbation process.

The solution procedure is described here only for plane crack growth problems with mode I stress intensity factor for the illustration of this method. Since the kernel function and the weight function are not specified in the equations, the ones derived here are general in form and suitable for various mode I crack problems. For mixed mode problems, since the integral equations are well established (Lee et al., 1987; Hanson et al., 1989), the perturbation equation can be derived by the same procedure although the resulting formulae will be more complicated. The only difference between the mixed mode crack and the mode I crack is the modification of eqn (17) to the following:

$$\delta E = 0, \quad \delta a \neq 0 \quad \text{if } E = E_c;$$
$$\delta E \neq 0, \quad \delta a = 0 \quad \text{if } E < E_c. \tag{18}$$

where δE is the variation of energy release rate which can be evaluated from the variation of stress intensity factors. For first order perturbation analysis a linear relation between δE and the variation of stress intensity factors δK_I, δK_{II} and δK_{III} can be derived, which is incorporated with the linear equation (16) to determine the unknown crack front node advance.

APPLICATIONS

In this section the perturbation method is illustrated by calculating the yield zone growth of a Dugdale-type crack under an increasing tensile load. The boundary conditions applied here are related for simplicity to the tensile yield stress alone rather than the maximum shear stress (Keer and Mura, 1965). The Dugdale model was proposed to deal with the problem of infinite stress at the crack tip involved in the elastic solution. Incidentally, this stress singularity does not present any difficulty for the solution of either the boundary element equation, eqn (2), or the perturbation equation (8), derived from it, for the unknown function in these equations is the crack opening displacement, which is finite at the edge of the crack.

In polar coordinates the initial planar crack shape is specified by $r = R_1(\theta)$, which upon loading is extended by a yield zone with front $r = R_2(\theta)$. The loading state for the area $r \leqslant R_1(\theta)$ is assumed to arise from a combination of a uniform tensile stress σ_0 and a stress having a linear variation, $\sigma_1 x/a$, i.e. $p = \sigma_0 + \sigma_1 x/a$, where a is a characteristic length of the crack geometry. The load in the yield zone $R_1(\theta) \leqslant r \leqslant R_2(\theta)$ is the sum of the loads σ_0, $\sigma_1 x/a$ and the yield stress σ_Y: $p = -\sigma_Y + \sigma_0 + \sigma_1 x/a$. The fracture criterion at the fictitious crack front $r = R_2(\theta)$ is that the stress intensity factor should be equal to zero, $K = 0$.

For a penny-shaped crack with $R_1 \equiv a$, $R_2 \equiv b$ under uniform load ($\sigma_1 = 0$), there exists an analytical solution (Tada et al., 1985) and the yield zone is specified by the equation:

$$\frac{R_1}{R_2} = \sqrt{1 - \frac{\sigma_0^2}{\sigma_Y^2}}. \tag{19}$$

To our knowledge there is still not an established method to determine the yield zone of Dugdale type cracks for general crack shapes and loading conditions.

The circular crack of unit radius: $R_1 \equiv 1$ subjected to loads having a linear variation

as specified above with $a = 1$ is considered first. The fictitious crack front is no longer circular and will be computed by the perturbation procedure described in this paper.

The perturbation is started from an initial circular fictitious crack front $R_2(\theta) \equiv C$ for which the stress intensity factor $K(\theta) \neq 0$. The crack front displacement δa at each step is determined by solving eqn (16) where δK is specified as $-\alpha K_s$. The value for α is chosen such that the maximum node displacement at each step is less than 0.03 to ensure the accuracy. After several perturbation steps, the stress intensity factor is reduced to such a level that it is approximately zero, considering the error associated with the solution of the original boundary element equation. In the present computation $K < 0.008$ is considered sufficiently small to be considered zero. At this stage the fictitious crack front is considered to have been found.

At the next stage, the uniform load σ_0 is allowed to increase, forcing the yield zone to grow. Suppose that the stress intensity factor produced solely by σ_0 without other loads present is K_0, which can be solved from eqn (2). The increment $\Delta\sigma_0$ in the uniform load will cause the stress intensity factor to increase by the amount $K_0\Delta\sigma_0/\sigma_0$. The advance of the crack front δa caused by the increment of the uniform load is solved from eqn (16) by prescribing δK as $-K_0\Delta\sigma_0/\sigma_0$, thus ensuring that the stress intensity factor remains unchanged after the growth. At each step the increment in the uniform load $\Delta\sigma_0$ is chosen such that the maximum node displacement is less than 0.03.

Numerical results for two different linear load magnitudes σ_1 are displayed in Figs 1–3, where the uniform load σ_0 and the linear variation load σ_1 is normalized by the yield stress σ_Y, which is of unit magnitude. In Fig. 3 the curve representing the analytical solution is obtained from eqn (19). It can be seen that the numerical results ($\sigma_1 = 0$) agree well with the known analytical solution.

In Figs 1 and 2 (also in Figs 4 and 5), where because of the symmetry only the upper half of the crack geometry is shown, the thicker solid line represents the real crack front while the other curves give the fictitious crack front at different stages of growth, corresponding to an increasing uniform stress level. Figure (3) shows the growth of the yield zone width at $\theta = 0$ ($x > 0$, $y = 0$) and $\theta = \pi$ ($x < 0$, $y = 0$) for different magnitudes of linear variation of stress levels. It is observed from these figures that due to the linear variation of stress the yield zone at $\theta = 0$ grows much faster than that at $\theta = \pi$. This phenomenon becomes more significant as the magnitude of the linear stress variation σ_1 increases.

The second case to be considered is the growth of the yield zone of a crack initially of elliptical shape subjected to the uniform tensile load only, i.e. $\sigma_1 = 0$. Considering the distribution of stress intensity factor around an elliptical crack, the growth of a yield zone
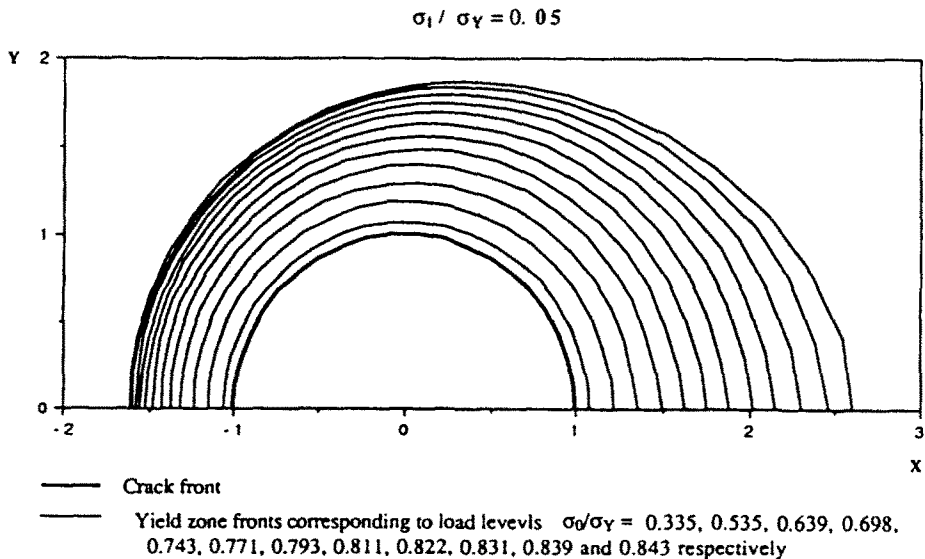
$$\sigma_1 / \sigma_Y = 0.05$$

Crack front

Yield zone fronts corresponding to load levevls $\sigma_0/\sigma_Y = 0.335, 0.535, 0.639, 0.698, 0.743, 0.771, 0.793, 0.811, 0.822, 0.831, 0.839$ and 0.843 respectively

Fig. 1. Growth of yield zone of Dugdale-type crack subjected to linear variation load.

$$\sigma_1 / \sigma_Y = 0.1$$

Crack front

Yield zone fronts corresponding to load levels $\sigma_0/\sigma_Y = $ 0.363, 0.526, 0.610, 0.661, 0.697, 0.719, 0.736, 0.746, 0.753 and 0.758 respectively
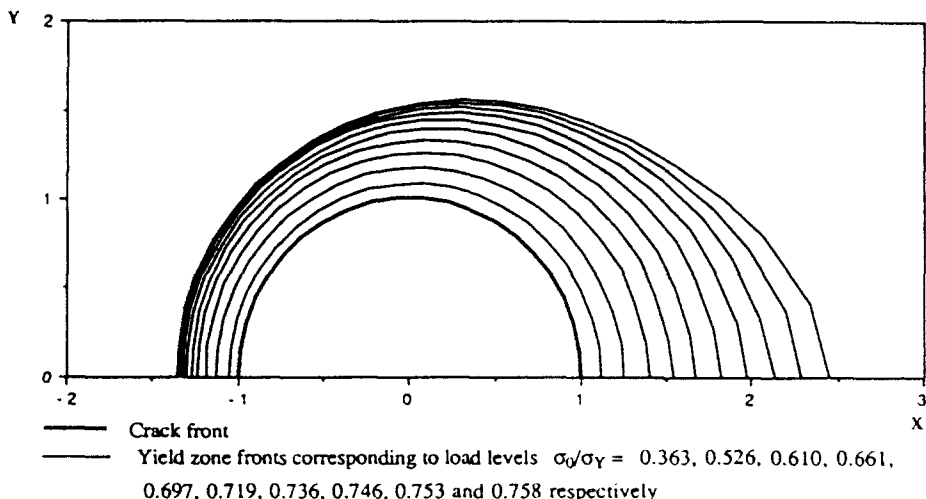
Fig. 2. Growth of yield zone of Dugdale-type crack subjected to linear variation load.

should eventually be almost circular. The real crack front is specified by $x = a \cos \theta$, $y = b \sin \theta$, and the yield zone is to be determined. The perturbation procedure to solve this problem is similar to that for the first case and begins from a fictitious crack front: $x = (a + \varepsilon) \cos \theta$, $y = (b + \varepsilon) \sin \theta$. After the actual fictitious crack front is found for the initial uniform tensile load level, σ_0 is increased. The results of the corresponding growth of the yield zone are presented in Figs 4–8, where the major semi-axis a is equal to 1.

Figures 4 and 5 show the gradual advance of the yield zone front accompanying the increase of the uniform load for cracks of elliptical shape with the ratio of minor to major semi-axis b/a equal to 0.8 and 0.6, respectively. The ratio of the maximum to minimum stress intensity factor along the elliptical crack front increases with the decrease of the ratio b/a. Numerical results display the feature that the fictitious crack becomes more circular as can be seen in Figs 4–8. By comparing Figs 6, 7 and 8, it is clear that when the ratio b/a becomes smaller the difference between the width of the yield zone at $\theta = 0$ and $\pi/2$ is
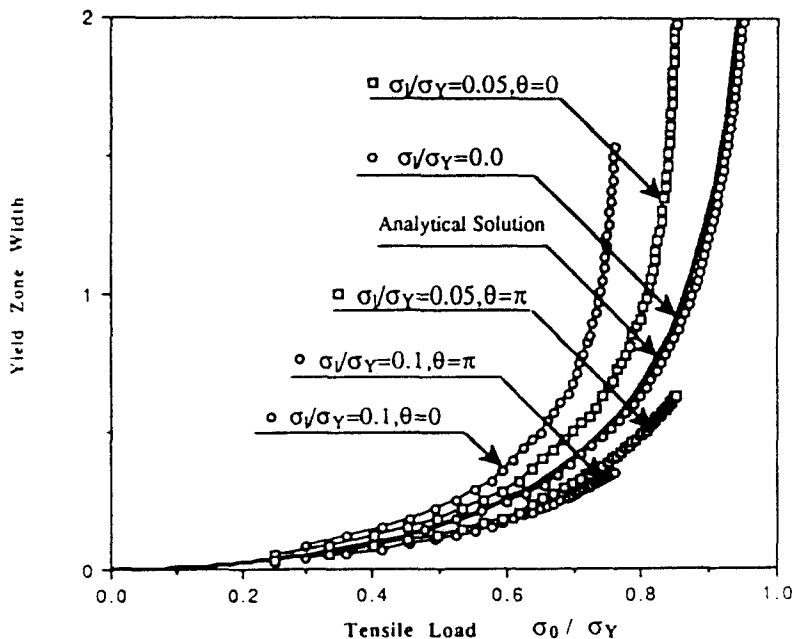

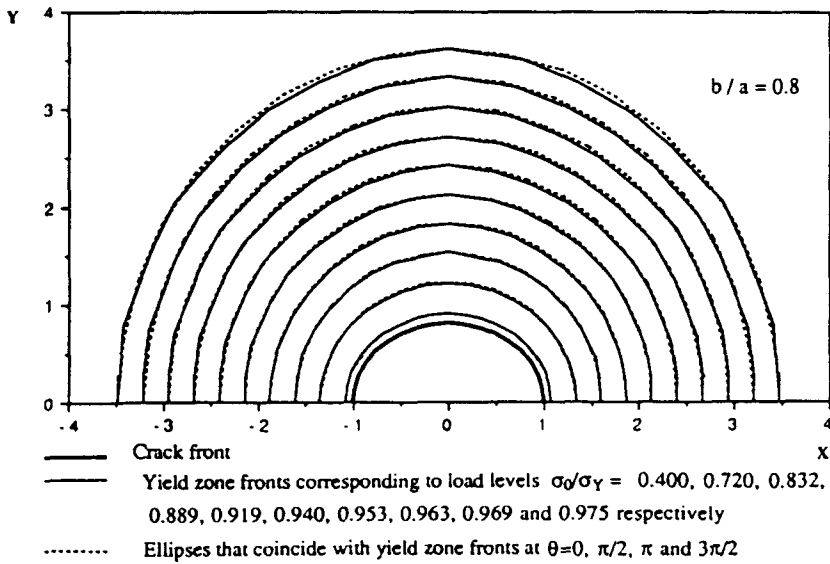Fig. 3. Growth of yield zone width vs increasing tensile load.

Fig. 4. Growth of yield zone of elliptical Dugdale-type crack.

greater. The difference also increases with the growth of the yield zone or the build up of the uniform tensile load. (The two curves in Figs 6–8 seem to merge as σ_0 increases. However, the difference between the two curves at a certain uniform load level is actually increasing.)

The dashed lines in Figs 4 and 5 represent the ellipses that coincide with the fictitious crack fronts at $\theta = 0$, $\pi/2$, π and $3\pi/2$. It is noted that the difference between the fictitious crack front and the corresponding ellipse is very small compared to the size of the yield zone. This observation raises the question of whether the fictitious crack front of elliptical Dugdale model cracks is still of elliptical shape. Although this point cannot be judged by the results of numerical analysis because there are unavoidable small errors, it can be concluded from the results that an ellipse that gradually approaches a circle is at least a good approximation of, if not the exact, shape of the fictitious crack front of elliptical Dugdale cracks.

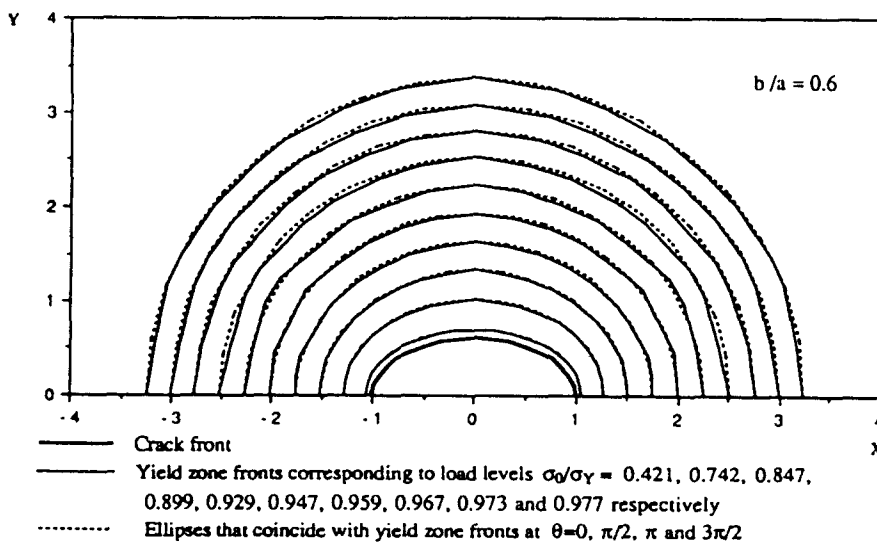It should be pointed out here that the prescribed load condition in the yield zone

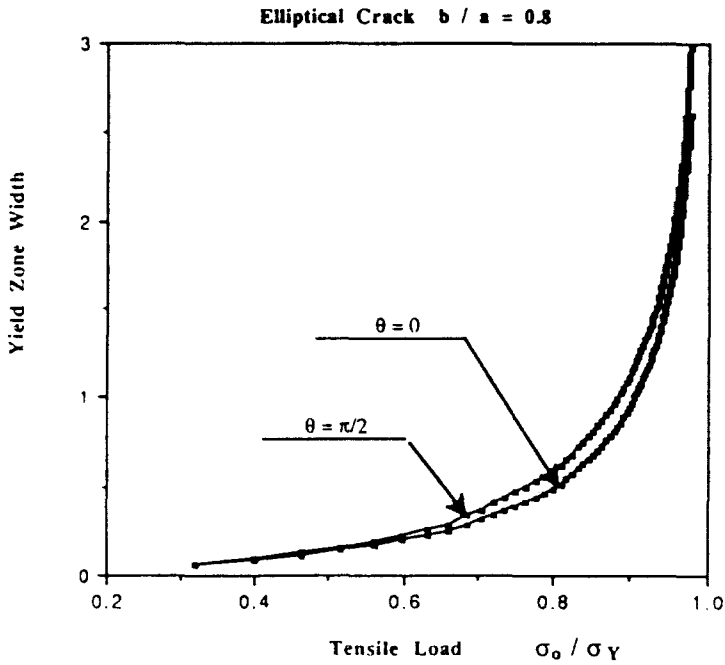Fig. 5. Growth of yield zone of elliptical Dugdale-type crack.

Elliptical Crack   b / a = 0.8

Fig. 6. Growth of yield zone width vs increasing tensile load.

implies the yield condition $\sigma_\cdot = \sigma_y$. Although this simple model has been adopted in many works done so far on three-dimensional Dugdale-type crack problems, a more strict analysis of this kind of problem should incorporate some established yield condition for the plastic zone such as the Tresca yield condition (Keer and Mura, 1965). Their results show that, in contrast to eqn (19), the relation between the width of the yield zone and the applied load depends on the Poisson's ratio of the material. Since the goal of the present paper was the demonstration of a direct method for calculation of crack growth, such cases are reserved for future investigations.
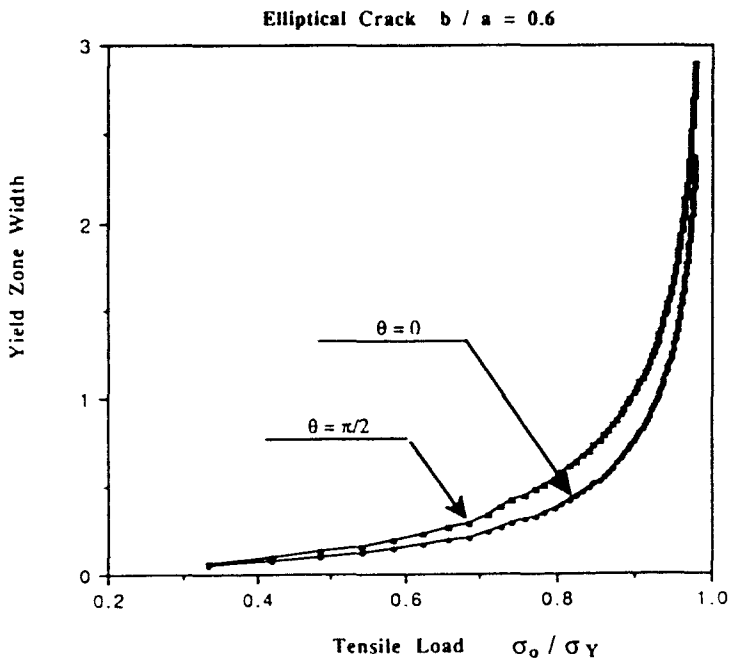
Elliptical Crack   b / a = 0.6

Fig. 7. Growth of yield zone width vs increasing tensile load.
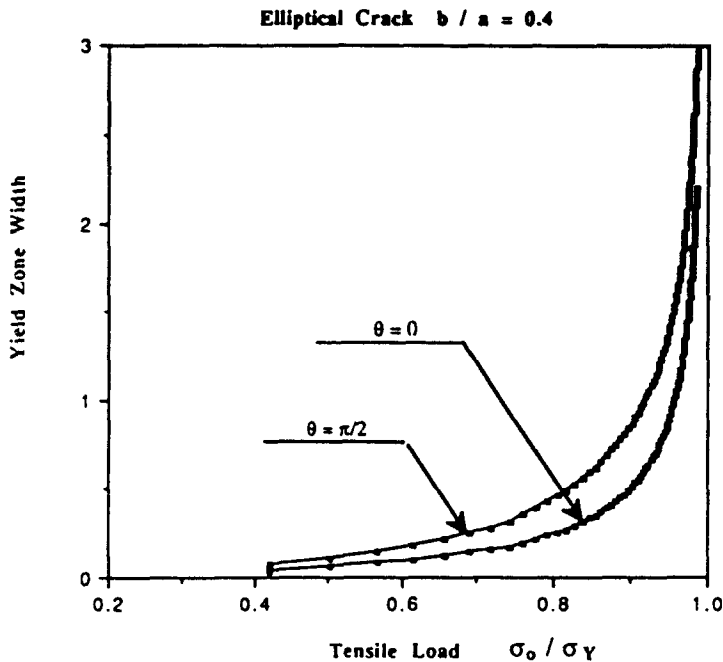
Elliptical Crack b / a = 0.4

Fig. 8. Growth of yield zone width vs increasing tensile load.

REFERENCES

Bertero, M., Mol, C. De and Pike, E. R. (1985). Linear inverse problems with discrete data. 1: General formulation and singular systems analysis. *Inverse Problems* 1(4), 301–330.

Bower, A. F. and Ortiz, M. (1990). Solution of crack problems by a finite perturbation method. *J. Mech. Phys. Solids* 38, 443–480.

Fares, N. (1989). Crack fronts trapped by arrays of obstacles: Numerical solutions based on surface integral representation. *J. Appl. Mech.* 56, 837–843.

Gao, H. and Rice, J. R. (1986). Shear stress intensity factors for a planar crack with slightly curved front. *J. Appl. Mech.* 53, 774–778.

Gao, H. and Rice, J. R. (1987). Somewhat circular tensile cracks. *Int. J. Fract.* 33, 155–174.

Gao, H. and Rice, J. (1989). A first-order perturbation analysis of crack trapping by arrays of obstacles. *J. Appl. Mech.* 56, 828–836.

Hanson, M. T., Lin, W. and Keer, L. M. (1989). Three-dimensional analysis of cracking through the boundary of a two-phase material. *J. Appl. Mech.* 56, 850–857.

Keer, L. M. and Mura, T. (1965). Stationary crack and continuous distributions dislocations. *Proc. First Int. Conf. on Fracture* Vol. 1, pp. 99–115. Published under the auspices of the Unified Research Society for Micro and Macro Mechanical Behavior of Materials and The Japan Society for the Promotion of Science. Edited by T. Yokobori, T. Kawasalei and J. L. Swedlow.

Keer, L. M., Nemat-Nasser, S. and Oranratnachai, A. (1978). Unstable growth of thermally induced interacting cracks in brittle solids: Further results. *Int. J. Solids Structures* 15, 111–126.

Lee, J. C., Farris, T. N. and Keer, L. M. (1987). Stress intensity factors for cracks of arbitrary shape near an interfacial boundary. *Engng Fract. Mech.* 27, 27–41.

Lee, J. C. and Keer, L. M. (1986). Study of a three-dimensional crack terminating at an interface. *J. Appl. Mech.* 53, 311–316.

Li, X. and Keer, L. M. (1992). The growth of pressurized planar cracks between barriers. *Int. J. Solids Structures* 29, 27–39.

Lin, W. and Keer, L. M. (1987). Scattering by a planar three-dimensional crack. *J. Acoust. Soc. Am.* 82, 1442–1448.

Mastrojannis, L. M., Keer, L. M. and Mura, T. (1980). Growth of planar cracks induced by hydraulic fracturing. *Int. J. Numer. Meth. Engng* 15, 41–54.

Nemat-Nasser, S., Keer, L. M. and Parihar, K. S. (1978). Unstable growth of thermally induced interacting cracks in brittle solids. *Int. J. Solids Structures* 14, 409–430.

Rice, J. R. (1985). First order variation in elastic fields due to variation in location of a planar crack front. *J. Appl. Mech.* 52, 571–579.

Rice, J. R. (1987). Weight function theory for three-dimensional elastic crack analysis. In *Fracture Mechanics*:

Perspectives and Directions, Twentieth Symposium (Edited by R. P. Wei and R. P. Gangloff), pp. 29–57. ASTM-STP-1020, American Society for Testing and Materials, Philadelphia.

Tada, H., Paris, P. C. and Irwin, G. R. (1985). *The Stress Analysis of Cracks Handbook* (2nd edn). Paris Production, St Louis.

Theocaris, P. S., Ioakimidis, N.I. and Kazantzakis, J. G. (1980). On the numerical evaluation of two-dimensional principal value integrals. *Int. J. Numer. Meth. Engng* 15, 629–634.

APPENDIX

For mode I crack problems, the singular part of the kernel has the form:

$$K'(x, x_0) = \frac{\mu}{4\pi(1-\nu)} \frac{1}{(\sqrt{(x-x_0)^2 + (y-y_0)^2})^3} = \frac{\mu}{4\pi(1-\nu)} \frac{1}{R^3}. \tag{A1}$$

In this appendix we give the formulae to calculate the derivatives of the finite part integral with respect to the positions of the collocation point and the nodal points. The finite part integral is in the form:

$$I = \text{F.P.} \int \frac{1}{R^3} \, dA. \tag{A2}$$

where the intgration is over the triangular element of nodes x_1, x_2 and x_3 with collocation point at x_0. By choosing a local (η, ξ) coordinate with the origin at x_0 and the η axis parallel to $x_1 x_2$, Lin and Keer (1987) have shown that

$$I = \frac{1}{\xi_1}\left(\frac{\gamma_{01}}{\beta_1} - \frac{\gamma_{01}}{\beta_2}\right) - \frac{1}{\xi_2}\left(\frac{\gamma_{01}}{\beta_1} - \frac{\gamma_{02}}{\beta_2}\right). \tag{A3}$$

where

$$\gamma_{0i} = |x_0 - x_i|, \quad \beta_i = \eta_1 - \xi_1(\eta_1 - \eta_i)/(\xi_1 - \xi_i).$$

The local coordinate (η_i, ξ_i) of the ith node is related to the global coordinate (x_i, y_i) through

$$\eta_i = (x_i - x_0)\cos\theta + (y_i - y_0)\sin\theta, \tag{A4}$$

$$\xi_i = -(x_i - x_0)\sin\theta + (y_i - y_0)\cos\theta, \tag{A5}$$

where

$$\sin\theta = \frac{y_2 - y_1}{\sqrt{(x_2 - x_1)^2 + (y_2 - y_1)^2}}, \tag{A6}$$

$$\cos\theta = \frac{x_2 - x_1}{\sqrt{(x_2 - x_1)^2 + (y_2 - y_1)^2}}. \tag{A7}$$

The derivatives of I with respect to x_0, x_1, x_2 and x_3 have the form:

$$\frac{\partial I}{\partial x_i} = \sum_{j=1}^{3}\left(\frac{\partial I}{\partial \xi_j}\frac{\partial \xi_j}{\partial x_i} + \frac{\partial I}{\partial \eta_j}\frac{\partial \eta_j}{\partial x_i}\right), \tag{A8}$$

$$\frac{\partial I}{\partial y_i} = \sum_{j=1}^{3}\left(\frac{\partial I}{\partial \xi_j}\frac{\partial \xi_j}{\partial y_i} + \frac{\partial I}{\partial \eta_j}\frac{\partial \eta_j}{\partial y_i}\right), \tag{A9}$$

In the above equations $\frac{\partial \xi_j}{\partial x_i}$, $\frac{\partial \xi_j}{\partial y_i}$, $\frac{\partial \eta_j}{\partial x_i}$ and $\frac{\partial \eta_j}{\partial y_i}$ are calculated from (A4)–(A7) whereas $\frac{\partial I}{\partial \xi_j}$ and $\frac{\partial I}{\partial \eta_j}$ are as follows:

$$\frac{\partial I}{\partial \xi_1} = \frac{1}{\beta_1^2}\left(\frac{\gamma_{01}}{\xi_1} - \frac{\gamma_{01}}{\xi_1}\right)\frac{\xi_1(\eta_1 - \eta_1)}{(\xi_1 - \xi_1)^2} - \frac{1}{\beta_2^2}\left(\frac{\gamma_{01}}{\xi_1} - \frac{\gamma_{02}}{\xi_2}\right)\frac{(\eta_1 - \eta_2)}{(\xi_1 - \xi_2)} + \frac{1}{\xi_1^2}\left(\frac{\gamma_{01}}{\beta_1} - \frac{\gamma_{02}}{\beta_2}\right) - \frac{1}{\gamma_{01}\beta_1}, \tag{A10}$$

$$\frac{\partial I}{\partial \xi_2} = \frac{1}{\beta_2^2}\left(-\frac{\gamma_{01}}{\xi_1} + \frac{\gamma_{02}}{\xi_2}\right)\frac{\xi_1(\eta_1 - \eta_2)}{(\xi_1 - \xi_2)^2} + \frac{1}{\gamma_{02}\beta_2}, \tag{A11}$$

$$\frac{\partial I}{\partial \xi_1} = \frac{1}{\beta_1^2}\left(-\frac{\gamma_{01}}{\xi_1} + \frac{\gamma_{01}}{\xi_1}\right)\frac{\xi_1(\eta_1 - \eta_1)}{(\xi_1 - \xi_1)^2} + \frac{1}{\beta_2^2}\left(\frac{\gamma_{01}}{\xi_1} - \frac{\gamma_{02}}{\xi_2}\right)\frac{\xi_1(\eta_1 - \eta_2)}{(\xi_1 - \xi_2)^2} + \left(\frac{1}{\beta_1} - \frac{1}{\beta_2}\right)\left(\frac{1}{\gamma_{01}} - \frac{\gamma_{01}}{\xi_1}\right). \tag{A12}$$

$$\frac{\partial I}{\partial \eta_1} = \frac{1}{\beta_1^2}\left(-\frac{\gamma_{01}}{\xi_3} + \frac{\gamma_{01}}{\xi_1}\right)\frac{\xi_3}{\xi_3 - \xi_1} - \frac{\eta_1}{\xi_1 \gamma_{01}\beta_1}.$$ (A13)

$$\frac{\partial I}{\partial \eta_2} = \frac{1}{\beta_2^2}\left(\frac{\gamma_{03}}{\xi_3} - \frac{\gamma_{02}}{\xi_2}\right)\frac{\xi_3}{\xi_3 - \xi_2} + \frac{\eta_2}{\xi_2 \gamma_{02}\beta_2}.$$ (A14)

$$\frac{\partial I}{\partial \eta_3} = \frac{1}{\beta_1^2}\left(\frac{\gamma_{03}}{\xi_3} - \frac{\gamma_{01}}{\xi_1}\right)\frac{\xi_1}{\xi_3 - \xi_1} + \frac{1}{\beta_2^2}\left(-\frac{\gamma_{03}}{\xi_3} + \frac{\gamma_{02}}{\xi_2}\right)\frac{\xi_2}{\xi_3 - \xi_2} + \frac{\eta_3}{\gamma_{01}\xi_3}\left(\frac{1}{\beta_1} - \frac{1}{\beta_2}\right).$$ (A15)